

Melt densities in the CaO-FeO-Fe₂O₃-SiO₂ system and the compositional dependence of the partial molar volume of ferric iron in silicate melts

DONALD B. DINGWELL¹ and MARK BREARLEY^{2,*}

¹Bayerisches Geoinstitut, Universität Bayreuth, Postfach 10 12 51, D-8580 Bayreuth, West Germany

²Institute of Geophysics and Planetary Physics, University of California, Los Angeles, CA 90024, U.S.A.

(Received June 15, 1988; accepted in revised form September 15, 1988)

Abstract—The densities of 10 melts in the CaO-FeO-Fe₂O₃-SiO₂ system were determined in equilibrium with air, in the temperature range of 1200 to 1550°C, using the double-bob Archimedean technique. Melt compositions range from 6 to 58 wt% SiO₂, 14 to 76 wt% Fe₂O₃ and 10 to 46 wt% CaO. The ferric-ferrous ratios of glasses drop-quenched from loop fusion equilibration experiments were determined by ⁵⁷Fe Mössbauer spectroscopy.

Melt densities range from 2.689 to 3.618 gm/cm³ with a mean standard deviation from replicate experiments of 0.15%. Least-squares regressions of molar volume versus molar composition have been performed and the root mean squared deviation shows that a linear combination of partial molar volumes for the oxide components (CaO, FeO, Fe₂O₃ and SiO₂) cannot describe the data set within experimental error. Instead, the inclusion of excess terms in CaFe³⁺ and CaSi (product terms using the oxides) is required to yield a fit that describes the experimental data within error. The nonlinear compositional-dependence of the molar volumes of melts in this system can be explained by structural considerations of the roles of Ca and Fe³⁺.

The volume behavior of melts in this system is significantly different from that in the Na₂O-FeO-Fe₂O₃-SiO₂ system, consistent with the proposal that a proportion of Fe³⁺ in melts in the CaO-FeO-Fe₂O₃-SiO₂ system is not tetrahedrally-coordinated by oxygen, which is supported by differences in ⁵⁷Fe Mössbauer spectra of glasses. Specifically, this study confirms that the ⁵⁷Fe Mössbauer spectra exhibit an area asymmetry and higher values of isomer shift of the ferric doublet that vary systematically with composition and temperature (this study; DINGWELL and VIRGO, 1987, 1988). These observations are consistent with a number of other lines of evidence (e.g., homogeneous redox equilibria, DICKENSON and HESS, 1986; viscosity, DINGWELL and VIRGO, 1987, 1988). Two species of ferric iron, varying in proportions with temperature, composition and redox state, are sufficient to describe the above observations.

The presence of more than one coordination geometry for Fe³⁺ in low pressure silicate melts has several implications for igneous petrogenesis. The possible effects on compressibility, the pressure dependence of the redox ratio, and redox enthalpy are briefly noted.

INTRODUCTION

THE IMPORTANCE OF iron redox equilibria in the chemical and physical evolution of magmas is illustrated most clearly by the fact that significant (major element) abundances of both ferric and ferrous iron occur in the vast majority of igneous rocks. It is this polyvalent nature of iron, in the range of oxygen fugacities experienced by magmas during igneous petrogenesis, which records so much of the petrogenetic evolution of oxygen fugacity in the form of ferric-ferrous ratios of minerals and glasses. Accordingly, the discussion of iron in silicate melts of geological relevance has been largely one of the contrasting properties of ferric and ferrous iron in these melts and this discussion has generally assumed that ferric and ferrous iron may each be dealt with as a single component.

Much of the investigation of the structural role of ferric iron in silicate melts has been dedicated to determining whether ferric iron may be considered as a network-forming component of the aluminosilicate network which dominates the structure of igneous melts. Various structural investigations of silicate melts and (more commonly) glasses have consistently returned the result that ferric iron in alkali-silicate and alkali-aluminosilicate melts is tetrahedrally-coordinated by oxygen (BROWN *et al.*, 1979; DANCKWERTH and VIRGO,

1982; FOX *et al.*, 1982; FLEET *et al.*, 1984; HENDERSON *et al.*, 1984; GOLDMAN, 1986). The case for alkaline earth silicate and aluminosilicate melts is less clear (KURKJIAN and SIGETY, 1968; PARGAMIN *et al.*, 1972; LEVY *et al.*, 1976; MYSEN *et al.*, 1980; VIRGO and MYSEN, 1985).

Additionally, the case for substitution of ferrite tetrahedra into the network structure of (alumino)silicate melts remains unproven. The alternative possibility of a clustering of tetrahedrally-coordinated ferric iron to form an iron-rich substructure might have significant implications for important melt properties such as configurational entropy and component activities (e.g., activity of SiO₂). The possibility of an iron-rich substructure would also serve to obscure the assignment of ferric iron to tetrahedral coordination, using methods which record the effect of ferric iron on bulk melt properties such as the non-bridging oxygen population (e.g., ESCA spectra; GOLDMAN, 1986) or silica activity trends from phase equilibria (DICKENSON and HESS, 1986). This is because the influence of the coordination of ferric iron, in an iron-rich substructure, on properties such as $a(\text{SiO}_2)$, would be indirect.

This study of melt densities in the CaO-FeO-Fe₂O₃-SiO₂ system was prompted by the previous ⁵⁷Fe Mössbauer spectroscopic observation (e.g., MYSEN *et al.*, 1984, 1985; VIRGO and MYSEN, 1985) that a change in the value of isomer shift of ferric iron occurs as a function of composition (*i.e.* oxidation state, identity of alkali/alkaline earth cation) in simple silicate melts. The question posed herein is "Does the variable isomer shift of ferric iron in glasses quenched from silicate

* Present address: Bayerisches Geoinstitut, Universität Bayreuth, Postfach 10 12 51, D-8580 Bayreuth, West Germany.

Table 1. Starting compositions

Composition	Nominal			Analyzed		
	CaO	Fe ₂ O ₃	SiO ₂	CaO	Fe ₂ O ₃	SiO ₂
1	34.5	38.5	27.0	34.12 (0.61)	39.06 (0.66)	26.82 (0.71)
2	24.1	28.3	47.6	24.38 (0.11)	28.24 (0.25)	47.38 (0.43)
3	26.2	66.3	7.5			
4	15.5	44.0	40.5	15.63 (0.89)	44.16 (1.29)	40.11 (0.84)
5	20.2	58.0	22.0			
6	45.0	19.0	36.0	45.25 (0.17)	19.00 (0.13)	35.75 (0.44)
7	45.7	47.8	6.5			
8	29.5	14.0	56.5	30.36 (0.11)	14.44 (0.33)	55.70 (0.77)
9	11.0	55.0	34.0			
10	11.5	76.0	12.5			

Microprobe analyses using 15 kV accelerating voltage, 12 nA beam current and 20 micron raster. Standards were Grossular (Ca, Si) and Magnetite (Fe). Numbers in brackets are 1σ of six analyses. The analyses were performed on chips of 100g batches poured onto a steel plate, some inhomogeneity observed in the less siliceous samples is due to the difficulty of quenching these fluid samples.

melts have any implications for the partial molar properties of ferric iron measured *in silicate melts*?. Preliminary evidence for significantly different behavior of melt properties in Na- versus Ca-ferrosilicate melts was observed in the viscosity-redox studies of DINGWELL and VIRGO (1987, 1988). The density results of the present study, combined with those of DINGWELL *et al.* (1988) on the Na₂O-FeO-Fe₂O₃-SiO₂ system, confirm that the volume properties of ferric iron also differ between these two systems.

In view of this contrasting behavior and the fact that Na and Ca are both major components of igneous rocks we may

be faced with the task of treating ferric iron as two separate components in the description of the structure and the prediction of the properties of igneous melts.

EXPERIMENTAL METHOD

Sample preparation

The starting materials for the densitometry experiments were synthesized from CaCO₃ (ultrapure precip.—Merck), Fe₂O₃ (>99%—Merck) and SiO₂ (−325 mesh, 99.9%—Alfa-Ventron). CaCO₃ and Fe₂O₃ powders were dried at 120°C for 24 h and SiO₂ was fired at 1250°C for 1–2 h and all were stored in a desiccator prior to weighing. One hundred gram (decarbonated weight) batches of the oxide powders were weighed into a 250 ml plastic beaker, transferred to a plastic bottle and mixed by agitation for approximately 15 minutes. The powder mixes were fused directly at 1550°C by stepwise addition of powder to a 50 cm³ thin-walled platinum crucible. The melts were held at 1600°C for 1 hour in a MoSi₂ box furnace and were poured onto a stainless steel plate for cooling. The samples that quenched to glasses were analysed by electron microprobe for composition and homogeneity and the results of these analyses (all within error of the weighed-in compositions) are presented in Table 1. It is important to note that the high σ values of the probe analysis of sample 4 are due to inhomogeneity generated during the relatively slow quench (by 100 g batch pour) of this very fluid melt after densitometry. Melt inhomogeneity due to batch preparation is not significant as can be seen from the analyses of the more viscous (and therefore easier to quench) more iron-poor compositions of Table 1. It is these compositions that would be expected to show synthesis inhomogeneity, if it were significant. The mixture compositions are illustrated in Fig. 1 in the CaO-Fe₂O₃-SiO₂ system with the phase relations (in equilibrium with air) determined by PHILLIPS and MUAN (1959). Also

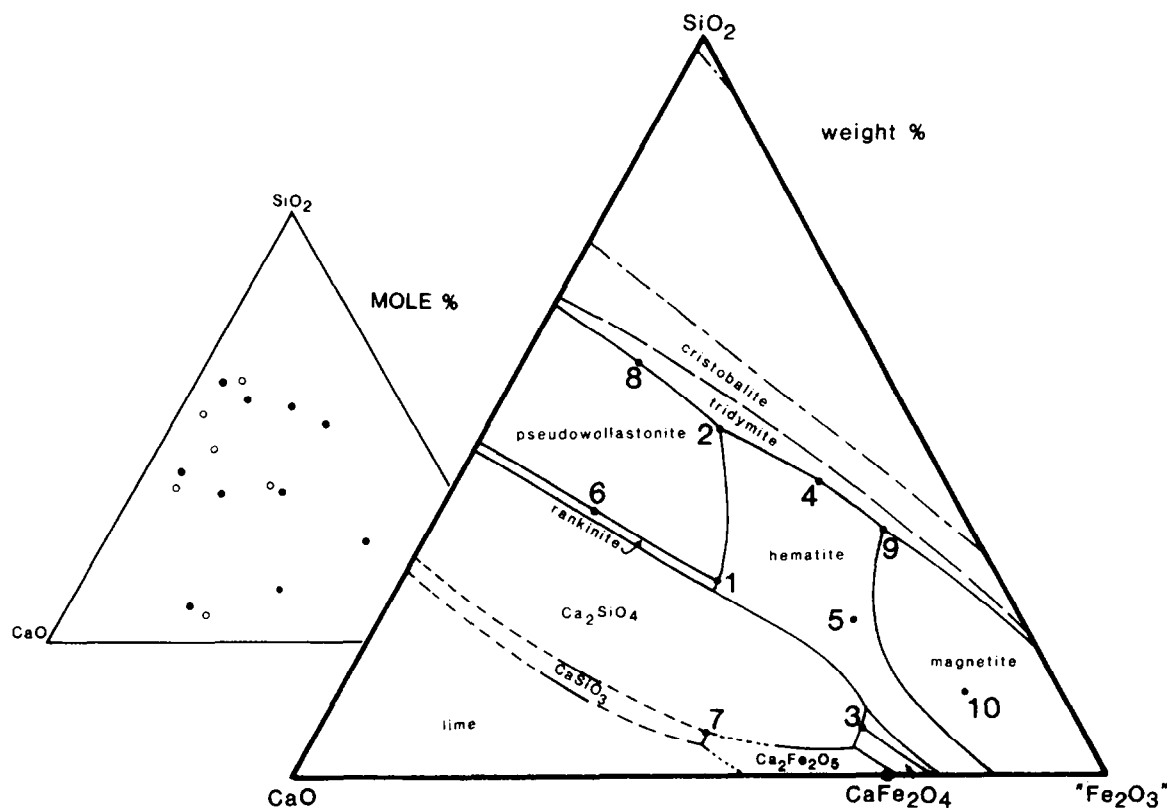


FIG. 1. The compositions of investigated melts (1–10) in the CaO-Fe₂O₃-SiO₂ system. The liquidus surface of CaO-FeO-Fe₂O₃-SiO₂ is taken from PHILLIPS and MUAN (1959). The mole% plot compares the range of compositions investigated in this study (solid dots) with those investigated by LANGE and CARMICHAEL (1987) (open dots) in the CaO-Al₂O₃-SiO₂ system.

included in Fig. 1 are the nominal compositions used in this study (inset) illustrating the large composition range accessible in this system. This accessible range is controlled by the temperature of the liquidus surfaces and is similar to that for the CaO-Al₂O₃-SiO₂ system (OSBORN and MUAN, 1960) but contrasts strongly with the relatively small ranges accessible in the Na₂O-FeO-Fe₂O₃-SiO₂ (DINGWELL *et al.*, 1988) and, especially, the Na₂O-Al₂O₃-SiO₂ system (STEIN *et al.*, 1986) where experiments on low SiO₂ compositions are impeded by Na volatilization and high liquidus temperatures (BOWEN *et al.*, 1930; SCHAIRER and BOWEN, 1956).

Densitometry

The melt densities were determined using the double-bob Archimedeian technique. The apparatus used has been illustrated previously (DINGWELL *et al.*, 1988). The fused starting materials were remelted in rigid, cylindrical Pt₉₀Rh₁₀ crucibles (2.54 cm inner dia., 5.08 cm height, 1 mm wall thickness) and bottom-loaded into a (3.5 cm inner diameter) vertical tube furnace. The samples were supported in the hot zone of the furnace by an alumina tube (2.54 cm outer diameter) pedestal. Hot zone temperature was maintained with an electronic set-point controller and a Pt₉₄Rh₆-Pt₇₀Rh₃₀ control thermocouple and monitored with a Pt-Pt₉₀Rh₁₀ measuring thermocouple (checked periodically against the melting point of gold). The measuring thermocouple was sheathed in a platinum sleeve and immersed in the sample before and after each density determination. We estimate the maximum temperature variation due to time fluctuations and thermal gradients to be $\pm 2^\circ\text{C}$. The tube furnace (MoSi₂ elements) is mounted on a screw jack which permits vertical positioning of the furnace and sample to a precision of 0.2 mm over a range of 15 cm. A table above the furnace supports a centering stage designed to position the balance over the furnace. The balance was tared prior to each immersion.

The bobs used for immersion were fabricated from platinum in the form of spindles. The bobs were suspended from 0.5 mm diameter platinum wire leaders which were, in turn, suspended from 1.0 mm diameter wire lengths that extended out of the furnace. The thin leaders minimize errors in immersed mass due to uncertainty in the immersed length of the leaders.

The masses of the bobs, corrected for air, were measured prior to this study and at regular intervals during the buoyancy determinations. The high temperature submerged volumes of the bobs were computed from their masses, a volume-temperature relationship for platinum and geometric considerations of the immersed length of leader wire and the melt height displacement of the submerged bob.

The experiments were conducted in sets of 6 separate immersions at each of three temperatures (generally ranging from the sample liquidus to 1550°C) for each composition. The large and small bobs were each immersed three times and a mean and standard deviation of the replicate buoyancy determinations was computed for each. Each reimmersion of the bobs involved all the intermediate steps required between different samples (*e.g.*, removing the wire and bob assembly, cleaning the bob in 40% HF, resuspending the bob and retaring the balance). Thus the (intrasample) precision obtained is a valid representation of the intersample precision. The mean buoyancies were entered into Eqn. (1) to solve for density.

$$\rho = (B_1 - B_2)/(V_1 - V_2) \quad (1)$$

where B_1 and B_2 are the buoyancies and V_1 and V_2 are the submerged volumes of the large and small bobs, respectively.

Precision and accuracy

The precision of the density determinations was obtained by propagating the standard deviations of the buoyancy determinations through Eqn. (1) using the square root of the sum of squares. The individual precisions are reported (in Table 2) for each temperature and composition and the mean of these is 0.15% of the measured density. This is within the range of the precisions obtained in a recent study of iron-free silicate densities (LANGE and CARMICHAEL, 1987) but better than the precision of previous workers in Fe-bearing melts (MO *et al.*, 1982; DINGWELL *et al.*, 1988). Previous observations of relatively low precision in density studies of Fe-bearing silicate melts

Table 2. Melt densities

Sample	Temp.	Density	Temp.	Density	Temp.	Density
1	1500	3.1034 (0.0038)	1366	3.1274 (0.0021)	1253	3.1693 (0.0044)
2	1500	2.8500 (0.0017)	1375	2.8834 (0.0089)	1260	2.8941 (0.0055)
3	1500	3.5504 (0.0103)	1375	3.5727 (0.0062)	1263	3.6135 (0.0027)
4	1550	3.0441 (0.0021)	1476	3.0584 (0.0039)	1382	3.0832 (0.0029)
5	1550	3.3729 (0.0061)	1475	3.3938 (0.0072)	1400	3.4041 (0.0054)
6	1550	2.8727 (0.0068)	1475	2.8954 (0.0046)	1400	2.9152 (0.0051)
7	1493	3.2463 (0.0010)	1433	3.2843 (0.0026)		
8	1554	2.6885 (0.0035)	1460	2.7013 (0.0057)	1380	2.7056 (0.0035)
9	1550	3.2312 (0.0068)	1501	3.2415 (0.0023)	1417	3.2469 (0.0048)
10	1553	3.6069 (0.0012)	1505	3.6179 (0.0043)		

Numbers in brackets are 1 σ precision.

(BOTTINGA *et al.*, 1983, 1984) and the relatively low quality of fits including Fe-bearing melts in the data base (LANGE and CARMICHAEL, 1987) have been attributed, in part, to uncertainties in composition associated with the determination of the redox state of the melt. The precision of this study obviates the need for uncertainties in the redox state as an explanation of the poor precision in such studies. Similarly, the results of this study indicate that at least some of the decrease in the quality of fit obtained when including Fe-bearing melts in the data base may be due to a compositional-dependence of the partial molar volume of Fe₂O₃ (see below).

The accuracy of this apparatus and technique was tested by DINGWELL *et al.* (1988). The density of molten NaCl was determined immediately prior to this study, at 1063°C, to be 1.4152 gm/cm³ in good agreement with the data of JANZ (1980) (0.19% higher). A redetermination at the end of this study yielded 1.4147 gm/cm³ (0.16% higher). Both of these determinations are within the mutual errors of the determinations. This redetermination illustrates that iron contamination was not a significant factor in bob density.

Redox characterization

The temperature-dependence of the ferric-ferrous ratio in these liquids was investigated using platinum loop equilibration experiments. Eighty \pm 10 mg of each composition were equilibrated with air at temperatures of 1400 and 1600°C for 1 hour. DINGWELL *et al.* (1988) used time series equilibrations to show that 1 hour is sufficient for equilibration of samples more viscous than those investigated here. The equilibrated samples were drop-quenched into water. Compositions 3, 7 and 10 could not be quenched to glasses and were discarded in subsequent analysis of the redox data (see below). The glassy drop-quenched samples were ground in an agate mortar and analysed for ferric-ferrous ratio by ⁵⁷Fe Mössbauer spectroscopy.

Resonant absorption ⁵⁷Fe Mössbauer spectra were collected at 25°C, with a 50 mCi ⁵⁷Co/Rh source, on powders contained between sheets of aluminum foil. The absorber thickness was constrained to yield approximately 5 mg Fe/cm². Mirror image spectra were recorded over 512 channels, folded and analyzed. The spectral data were deconvoluted with the least-squares fitting routine PC-MOS (copyright CMTE Elektronik, Riemerling, FRG) using Lorentzian lineshapes. The fitting procedure is discussed below. One sample that was unquenchable, composition 7, was retained in the subsequent treatment of the results of this study because the assumption of complete oxidation can be justified on the following grounds.

The results of phase equilibrium experiments in the CaO-FeO-Fe₂O₃-SiO₂ system by PHILLIPS and MUAN (1959) include contours of ferric/total iron in liquids along the liquidus surfaces. Composition 7 lies to the oxidized side of the 1% ferrous iron contour and thus contains less than 0.0025 mole fraction of ferrous iron at its liquidus temperature (1405°C). Additional evidence for extremely oxidized conditions in this compositional region come from the redox study of LARSON and CHIPMAN (1953) in the adjacent Fe-O-Si system.

Figure 7 of LARSON and CHIPMAN (1953) illustrates liquid compositions in the CaO-FeO-Fe₂O₃ system as a function of f_{O_2} at 1550°C. The projection of composition 7 from SiO₂ to the CaO-FeO-Fe₂O₃ system (only 6 wt%) yields a fully oxidized liquid composition along the $f_{O_2} = 0.2$ isopleth.

We wish to emphasize that we justify this estimate of the redox state of composition 7 based on the insignificant FeO content so derived. We do not feel justified in applying calculated ferric-ferrous ratios to quantify the ferrous iron content of moderately reduced samples. Thus calculations for compositions 3 and 10 (which would contain significant FeO by such methods) are not attempted. Inclusion of these compositions in the volume modelling presented below awaits better, faster quenching techniques.

RESULTS

Densities

The computed densities derived from 168 buoyancy measurements on 10 melt compositions are reported in Table 2 and shown in Fig. 2. The melt densities range from 2.689 to 3.618 gm/cm³ (a variation of 35%). There is a linear relationship between density and temperature for each composition within the uncertainty of the determinations (Fig. 2). The mean precision of the density determinations derived solely from the precision of replicate buoyancy determinations (as noted above) is 0.15%. The analytical errors involved in the microprobe analyses are estimated to be less than 1% relative for SiO₂, total iron and CaO. The errors in ferric/total iron derived from fits to the Mössbauer spectra are $\pm 2\%$. The temperature uncertainty propagates into a density imprecision of ± 0.0005 gm/cm³ using a mean specific expan-

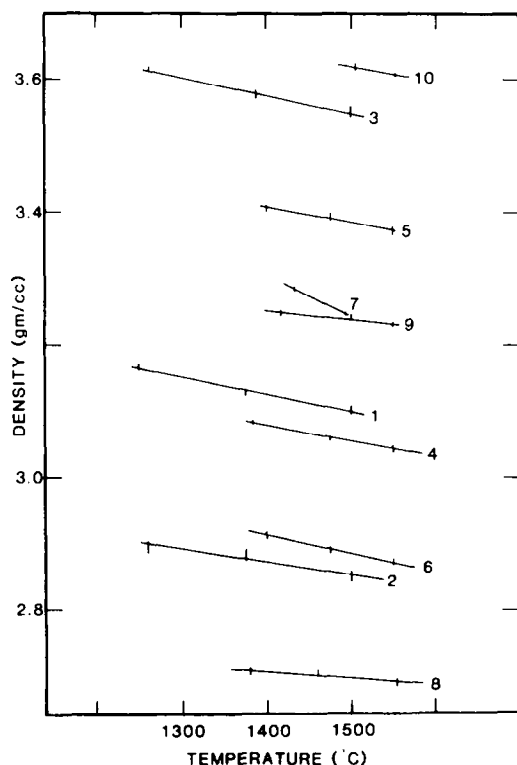


FIG. 2. The densities of melts in the CaO-FeO-Fe₂O₃-SiO₂ system determined in this study. For each composition the density data may be described as a linear function of temperature.

sivity of 2.5×10^{-4} gm/cm³ °C. The density measurements and melt compositions were used to calculate the molar volumes of the melts and the above errors propagate into a mean error of 0.34% (or 0.09 cm³/mole) in the molar volumes of the melts.

⁵⁷Fe Mössbauer spectra

⁵⁷Fe Mössbauer spectra of quench glasses in the CaO-FeO-Fe₂O₃-SiO₂ system have been described by several workers in the past (*e.g.*, FRISCHAT and TOMANDL, 1968; PARGAMIN *et al.*, 1972; MYSEN and VIRGO, 1983) and the Mössbauer spectra of quench glasses in this study are equivalent to those that have been previously obtained under similar conditions of bulk composition, oxygen fugacity and temperature. The cumulative envelopes of these spectra consist of three resolved peaks, two of which are in the positive velocity region, and therefore, at least two quadrupole split doublets are required to fit the spectral data. In the case of relatively oxidized glasses such as those observed in this study, the two lower velocity peaks are always larger than the highest velocity peak and, with decreasing quench temperature (and therefore more oxidized glasses), the relative intensities of the highest and lowest velocity peaks decrease. In accordance with this observed behavior the spectra of such glasses may be fitted to a low-velocity ferric iron doublet and a high-velocity ferrous iron doublet. In the initial fitting of these spectra to one ferric and one ferrous doublet, the fitting constraints of a symmetric ferric doublet (equal area, equal width) and an asymmetric ferrous doublet (equal area, unequal width) were employed. This was in accordance with the general observation of symmetric and asymmetric doublets for ferric and ferrous iron in many extremely oxidized and extremely reduced silicate glasses, respectively (MAO *et al.*, 1973; VIRGO and MYSEN, 1985). The results of the single symmetric ferric doublet fits are summarized in Table 3a and yield ferric isomer shifts that increase with quench temperature for each composition. The general quality of the fits is poor.

The composition-temperature range of this study produced some quench glasses that are extremely oxidized. The ⁵⁷Fe Mössbauer spectra of such a sample, composition 1 quenched from 1255°C, is illustrated in Fig. 3. The size of the ferrous doublet contribution to this spectrum is indicated by the high velocity shoulder which is barely visible; the low velocity ferrous peak must lie under the low velocity peak of the envelope. Despite the small contribution from this low velocity ferrous component, the low velocity peak in the envelope is lower and wider than that of the higher velocity peak in the envelope. The marked asymmetry of the envelope spectrum for this essentially fully-oxidized sample indicates that the ferric iron Mössbauer signal itself must be asymmetric in these glasses. The asymmetry of the ferric iron signal in these spectra was dealt with in three different ways for a number of the samples and a representative comparison of the results of the fits is reported in Table 3b.

The first adjustment to the fitting procedure was to release the equal width constraint on the ferric doublet. The resulting fits to spectra with one asymmetric doublet each for ferric and ferrous iron did not result in any significant improvement in χ^2 (Table 3b). The asymmetric ferric doublet was unable

Table 3a. Mössbauer data - 1 symmetric ferric doublet.

Sample/Temp. (°C)	Fe ³⁺ (IS)	Fe ³⁺ (QS)	Fe ²⁺ (IS)	Fe ²⁺ (QS)
1	1600	0.303	1.15	1.09
	1400	0.285	1.22	1.01
2	1600	0.359	1.05	0.92
	1400	0.307	1.16	0.95
4	1600	0.316	1.20	1.05
	1400	0.309	1.21	1.06
5	1600	0.362	0.95	1.06
	1400	0.294	1.13	0.96
6	1600	0.315	1.19	0.76
	1400	0.282	1.23	0.79
8	1600	0.341	1.04	0.96
	1400	0.299	1.15	1.00
9	1600	0.387	0.93	1.09
	1400	0.358	1.01	1.05

IS is isomer shift, QS is quadrupole splitting.

Table 3b. Comparison of Mössbauer fits (1-1400).

Ferric iron				Ferrous iron		χ ²
single symmetric				single asymmetric		
IS	QS			IS	QS	8.20
0.29	1.22			1.01	2.16	
single asymmetric						9.50
IS	QS			IS	QS	
0.28	1.24			0.90	2.13	
two symmetric (a)						2.81
IS	QS	IS	QS	IS	QS	
0.41	1.19	0.11	1.26	0.77	2.24	
(b)						2.45
0.27	1.49	0.32	0.85	0.78	2.15	

Table 3c. Mössbauer data - 2 ferric doublets.

Sample/Temp. (°C)	Fe ³⁺				Fe ²⁺		log(3+/2+)
	IS	QS	IS	QS	IS	QS	
1-1600	0.48	1.04	0.14	1.22	0.87	2.20	1.018
1-1400	0.41	1.19	0.11	1.26	0.77	2.24	1.602
1-1255	0.40	1.21	0.11	1.29	0.76	2.17	1.650
2-1600	0.44	1.12	0.17	1.19	1.02	1.97	0.295
2-1400	0.42	1.17	0.16	1.22	1.01	2.00	0.732
2-1220	0.39	1.22	0.13	1.26	1.01	2.00	1.264
4-1600	0.48	1.12	0.19	1.21	1.02	2.03	0.257
4-1400	0.43	1.18	0.16	1.24	1.02	2.03	0.672
5-1600	0.47	0.93	0.15	1.05	1.00	1.48	0.782
5-1400	0.40	1.12	0.15	1.23	0.80	1.67	0.949
6-1600	0.45	1.12	0.12	1.31	0.84	2.30	0.866
6-1400	0.43	1.17	0.11	1.30	0.83	2.32	1.230
8-1600	0.53	0.90	0.16	1.18	0.92	2.17	0.282
8-1400	0.48	1.04	0.17	1.22	0.90	2.23	0.781
9-1600	0.60	0.76	0.21	0.88	0.97	1.92	0.424
9-1400	0.55	0.83	0.15	1.12	0.87	1.90	0.556

to produce a lower velocity ferric doublet component with the area-width characteristics of the observed lower velocity peak (minus the ferrous contribution). The following four points led us to include a second ferric doublet in the fitting procedure: (1) failure of an asymmetric doublet to improve the quality of fit; (2) positive temperature-dependence of the ferric isomer shifts obtained in single symmetric ferric doublet fits (Table 3a); (3) contrasting behavior of glasses in the Na₂O-FeO-Fe₂O₃-SiO₂ system (where a symmetric ferric doublet suffices); and, (4) the observation that "fully" oxidized glasses

exhibit an asymmetry of the cumulative envelope and thus the asymmetry cannot be due to ferrous contributions.

The inclusion of a second ferric doublet in the fitting of Mössbauer spectra of glasses in the CaO-FeO-Fe₂O₃-SiO₂ system has been attempted in at least three previous studies. FRISCHAT and TOMANDL (1968) used two ferric doublets of similar quadrupole splittings and different isomer shifts to fit a series of glasses of varying Ca/Na ratio in the CaO-Na₂O-FeO-Fe₂O₃-SiO₂ system. In contrast, PARGAMIN *et al.* (1972), in a study that included "drop-smasher" quenching techniques, fit the ferric component of their spectra of CaO-FeO-Fe₂O₃-SiO₂ glasses to two symmetric ferric doublets of different quadrupole splittings and similar isomer shifts. Following the general observation of (VIRGO and MYSEN, 1985) of increasing ferric isomer shift (from single symmetric ferric doublet fits) with reduction of Fe-bearing alkali and alkaline earth silicate and aluminosilicate glasses, DINGWELL and VIRGO (1987, 1988) returned to the consideration of two ferric doublets of differing isomer shifts to fit the ⁵⁷Fe Mössbauer spectra of glasses in the Na₂O-FeO-Fe₂O₃-SiO₂ and CaO-FeO-Fe₂O₃-SiO₂ systems. In addition, KURKJIAN and SIGETY (1968) produced a series of mechanical mixtures of phosphate and silicate glasses with structural assignments of octahedral and tetrahedral ferric iron, respectively. The resultant spectra (see their Fig. 5c) consisted of one broad asymmetric doublet with a lower broader low-velocity component and a higher, narrower, high velocity component similar to those observed in the CaO-FeO-Fe₂O₃-SiO₂ glasses of this study.

As mentioned above, the spectra of this study were thus fitted using two ferric doublets in order to account for the asymmetry of the ferric iron contribution to these spectra. We tried both the PARGAMIN *et al.* (1972) assumption of similar isomer shifts and differing quadrupole splittings and the FRISCHAT and TOMANDL (1968) assumption of differing isomer shifts and similar quadrupole splittings. Both of the

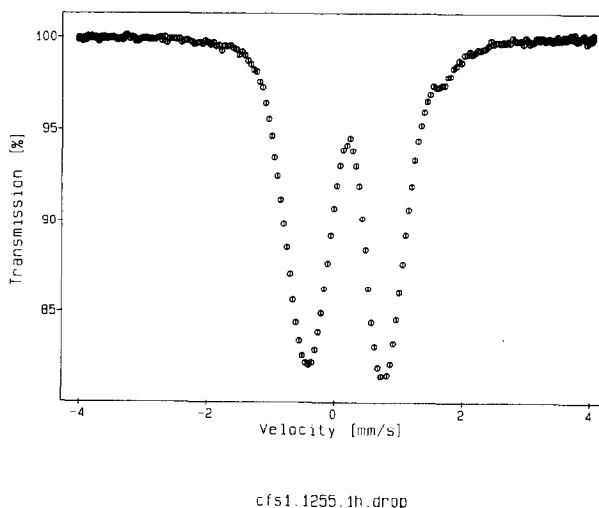


FIG. 3. ⁵⁷Fe Mössbauer spectrum of composition CFS 1. Spectrum collected at 298 K on a powder of a glass obtained by drop-quenching from an equilibration at 1255°C. Note the small ferrous iron contribution (the small, high velocity shoulder) and the strong asymmetry of the dominant, ferric iron contribution.

input assumptions returned fit spectra with significantly lower but similar values of χ^2 (e.g., Table 3b). We favor the latter (FRISCHAT and TOMANDL, 1968) input assumptions because the resulting components can be reconciled with two endmembers that dominate the ferric iron population in extremely oxidized and reduced alkali silicate (and alkali aluminosilicate) melts, respectively. In addition the two can mix to produce the full range of spectral signatures of ferric iron in alkali- and alkaline earth silicate and aluminosilicate melts (VIRGO and MYSEN, 1985; DINGWELL and VIRGO, 1987). The relative areas of the two ferric doublets have been interpreted by previous workers to indicate the proportions of octahedral and tetrahedral ferric iron in these melts (FRISCHAT and TOMANDL, 1968; PARGAMIN *et al.*, 1972; DINGWELL and VIRGO, 1987). Although we agree fully that these spectra are consistent with the presence of two ferric iron species whose proportions change with the bulk composition of the melt, we observe from our own experience of fitting the two symmetric ferric doublets to the spectra of this study that the precision in the area ratio of the two ferric component doublets is poor. Thus we do not wish, at this time, to attempt a quantitative estimate of the proportions of octahedral and tetrahedral ferric iron but rather to make some qualitative statements concerning reproducible trends in such proportions observed during the fitting. In general, we take the attitude that modelling the ^{57}Fe Mössbauer spectra of these glasses provides strong supportive evidence for a variable average coordination state of iron and that this variable state can be modelled successfully using two components (Table 3c). The spectra do not provide conclusive evidence of the exact polyhedral identity of these two ferric components. This density study of melts in the $\text{CaO-FeO-Fe}_2\text{O}_3\text{-SiO}_2$ system, however, is entirely consistent with a model involving two ferric iron species in these silicate melts (see below).

The redox ratio which is derived from the ^{57}Fe Mössbauer spectra is not significantly affected by the choice of the fitting method for the ferric iron doublet(s).

DISCUSSION

Partial molar volumes

The density data must be analyzed as a function of composition at individual temperatures (*cf.* MO *et al.*, 1982; LICKO *et al.*, 1985; Fe-bearing fits of LANGE and CARMICHAEL, 1987; DINGWELL *et al.*, 1988) because the redox ratio and, therefore, the chemical composition of each melt, changes as a function of temperature. This is the alternative to regressing the molar volumes of the individual compositions as functions of temperature as may be done in systems that do not involve redox equilibria (e.g., STEIN *et al.*, 1986). Also, because the density measurements of the melts in this study were performed at optimal temperatures dictated by the liquidus surface of the $\text{CaO-FeO-Fe}_2\text{O}_3\text{-SiO}_2$ system, we have derived linear temperature-density relationships from least-squares fits to the data set to permit interpolation of the density data at common temperatures of comparison. Figure 2 illustrates that the observed temperature-dependence of densities for melts in this system are linear within error (*cf.* LICKO *et al.*, 1985). The mole fractions of the four oxide components, CaO, FeO, Fe_2O_3 and SiO_2 were calculated from

the redox data of Table 3c and the compositional data of Table 1. The resulting molar compositions are presented in Table 4 for 1400, 1500 and 1600°C. The molar volume data were calculated from the molar composition data of Table 4 and the linear interpolations of the density data of Table 2 to yield the molar volumes presented in Table 4 for 1400, 1500 and 1600°C. The molar composition and volume data of Table 4 form the basic input data for the multilinear least-squares regressions of molar volume against composition. These regressions were performed on both linear and nonlinear combinations of the molar composition data, referred to below as linear and nonlinear fits, respectively. The results of the fits, linear and nonlinear, are presented in Table 5.

The linear fit equation is:

$$V = \sum_{i=1}^n X_i V_i \quad (2)$$

where V is the molar volume of the melt and X_i and V_i are the mole fraction and partial molar volume of the i th component, respectively. The nonlinear fit equations involve the addition of excess terms of the general form $X_j X_k V_{X_j X_k}$ (i.e., simple product terms of the endmember oxides whose mole fractions are denoted X_j and X_k) where $V_{X_j X_k}$ is termed the excess volume term,

$$V = \sum_{i=1}^n X_i V_i + X_j X_k V_{X_j X_k} \quad (3)$$

The selection of excess terms is discussed below. The partial molar volumes of the oxides are given in Table 5. The uncertainties in and the quality of these fits are indicated by the square root of the mean of squared residuals (RMSD), the standard errors of the fit coefficients (the volume terms) and by the significance of fit. The RMSD, when compared with our experimental uncertainty, indicates whether the fit can

Table 4. Fit Parameters.

Sample	X(CaO)	X(Fe_2O_3)	X(SiO_2)	X(FeO)	V^1
1400°C					
1	.4680	.1768	.3419	.0133	24.300
2	.3012	.1048	.5552	.0389	24.299
4	.2173	.1807	.5300	.0719	25.357
5	.3198	.2898	.3251	.0652	25.964
6	.5254	.0736	.3923	.0087	22.435
7	.6666	.2449	.0885	.0000	24.751
8	.3366	.0507	.6018	.0110	23.632
9	.1660	.2281	.4790	.1270	25.736
1500°C					
1	.4654	.1702	.3400	.0244	24.344
2	.2981	.0936	.5496	.0586	24.146
4	.2137	.1612	.5213	.1038	25.045
5	.3186	.2851	.3239	.0724	26.013
6	.5243	.0712	.3915	.0131	22.594
7	.6666	.2449	.0885	.0000	25.235
8	.3347	.0447	.5984	.0222	23.546
9	.1646	.2179	.4750	.1425	25.568
1600°C					
1	.4615	.1603	.3371	.0410	24.299
2	.2947	.0810	.5433	.0810	23.961
4	.2098	.1399	.5117	.1385	24.677
5	.3175	.2806	.3228	.0791	26.066
6	.5228	.0682	.3904	.0186	22.736
7	.6666	.2449	.0885	.0000	25.738
8	.3321	.0363	.5936	.0380	23.396
9	.1633	.2083	.4712	.1571	25.414

¹ all volumes in cm^3/gfw

Table 5. Fit results - Partial molar volumes.

Fit/Temp	V(CaO)	V(Fe ₂ O ₃)	V(SiO ₂)	V(FeO)	V(ex)	RMSD	Sig.
linear							
1400°C	19.24 (1.11)	38.36 (2.61)	24.78 (0.76)	14.40 (7.02)	-	0.64	2.12E-8
1500°C	20.27 (1.42)	37.53 (3.21)	24.27 (1.17)	17.77 (7.91)	-	0.74	3.93E-8
1600°C	21.53 (1.49)	36.38 (3.21)	23.35 (1.49)	21.58 (7.40)	-	0.82	5.87E-8
CaSi							
1400°C	20.79 (0.42)	36.90 (0.84)	27.80 (0.54)	10.42 (2.26)	-10.37 (1.66)	0.17	5.03E-8
1500°C	21.70 (0.36)	36.82 (0.72)	28.51 (0.55)	10.21 (1.96)	-12.93 (1.47)	0.14	2.98E-8
1600°C	22.94 (0.53)	35.89 (1.02)	28.54 (0.98)	12.62 (2.77)	-14.65 (2.42)	0.22	1.16E-7
CaFe ³⁺							
1400°C	16.80 (0.15)	27.16 (0.57)	26.30 (0.10)	24.29 (0.79)	27.98 (1.29)	0.05	1.31E-9
1500°C	17.46 (0.25)	27.12 (0.76)	25.88 (0.18)	24.14 (1.06)	28.48 (1.78)	0.08	5.19E-9
1600°C	17.76 (0.55)	29.65 (1.08)	25.76 (0.44)	25.76 (1.71)	20.76 (3.10)	0.17	4.45E-8
CaSi & CaFe ³⁺							
1400°C	17.35 (0.65)	28.44 (1.59)	26.54 (0.29)	22.40 (2.32)	-1.49/24.27 (1.72/4.48)	0.04	1.15E-6
1500°C	18.89 (0.50)	30.32 (1.17)	26.83 (0.34)	19.37 (1.72)	-4.54/19.02 (1.55/3.37)	0.03	7.53E-7
1600°C	19.82 (0.74)	32.02 (0.96)	27.08 (0.49)	17.19 (1.47)	-6.36/16.28 (2.09/3.70)	0.07	2.96E-6

volumes in cm³/gfw

adequately reproduce the volume data within our best estimate of experimental uncertainty. The significance of fit is the probability value derived from a comparison of *F* tests. Because the degrees of freedom of the fits are taken into consideration in the calculation of the *F*-value, the significance of fit can be used as a direct comparison of the relative statistical significance of fits with varying numbers of parameters. A lower significance means a higher degree of confidence of the significance of the coefficients of fit.

The linear fit

The linear fits at 1400, 1500 and 1600°C yield the partial molar volumes for the oxide components that are listed in lines 1 to 3 of Table 5. The RMSD of the linear fit at 1400, 1500 and 1600°C is 0.64, 0.74 and 0.82 cm³/mole. These values can be compared with our best estimate of experimental uncertainty. An estimate of 0.35% uncertainty in density determinations translates into a molar volume uncertainty (using a mean molar volume of 24.56 cm³/mole) of 0.09 cm³/mole.

The linear fit does not reproduce the experimental volume data within experimental error. The RMSD is too large at 1400, 1500 and 1600°C by factors of 7 to 9. Despite the inadequacy of the linear fit in describing the volume data of this study (Table 5, fit 1), the results form a useful comparison with previous linear fits to data from related systems. Firstly, it should be noted that the partial molar volume of Fe₂O₃ derived in these linear fits is within error of that obtained for the Na₂O-FeO-Fe₂O₃-SiO₂ system (DINGWELL *et al.*, 1988) (*e.g.*, at 1500°C, 37.53 ± 3.21 cm³/mole versus 40.71 ± 0.90 cm³/mole). Secondly, a negative thermal expansivity of Fe₂O₃ is generated by the linear fits in both the CaO-FeO-Fe₂O₃-

SiO₂ and the Na₂O-FeO-Fe₂O₃-SiO₂ systems. The negative thermal expansivity of SiO₂ generated in the CaO-FeO-Fe₂O₃-SiO₂ system suggests that the problem of low or zero thermal expansivity of SiO₂ in multicomponent linear fits, in general, may be an artifact of the linear fitting, because a reasonable, positive thermal expansivity has been measured for liquid SiO₂ (despite the large errors associated with those measurements, see BACON *et al.*, 1960).

If we compare the partial molar volumes derived for Fe₂O₃ from these linear fits to the CaO-FeO-Fe₂O₃-SiO₂ and Na₂O-FeO-Fe₂O₃-SiO₂ systems to the molar volume of octahedrally-coordinated, ferric iron in crystalline Fe₂O₃ at 1400°C (as has been done by previous investigators, *e.g.*, MO *et al.*, 1982; LANGE and CARMICHAEL, 1987) we obtain molar volumes for Fe₂O₃ that are 20% and 27% larger, respectively. Similarly, linear fits to the volume data in the CaO-Al₂O₃-SiO₂ (LANGE and CARMICHAEL, 1987) and Na₂O-Al₂O₃-SiO₂ (STEIN *et al.*, 1986) systems yield *V*(Al₂O₃) values that are 31% and 39% larger, respectively, than the 1400°C value for crystalline Al₂O₃. Thus, although we have demonstrated the inadequacy of the linear fit in describing the CaO-FeO-Fe₂O₃-SiO₂ volume data, the partial molar volumes derived from such a fit could lead to the assumption that the value of *V*(Fe₂O₃) obtained from the linear fit indicates tetrahedral coordination of iron in melts in this system. In fact, what the value of *V*(Fe₂O₃) represents is a weighted average of the volumes of two or more types of ferric iron coordination whose proportions may change with composition. In this case the linear fit is serving to obscure the difference in the coordination of ferric iron between the CaO-FeO-Fe₂O₃-SiO₂ and Na₂O-FeO-Fe₂O₃-SiO₂ systems.

Non-linear fits

A series of nonlinear fits of the molar volume data were attempted in order to bring the RMSD of the fits within the experimental error limits. Fits using simple binary product terms (*e.g.*, *X*_{CaO}*X*_{SiO₂} denoted CaSi) were generally unsuccessful. The inclusion of an Fe³⁺Si excess term yielded no significant improvement but the results of fits including CaSi and CaFe³⁺ excess terms (Table 5) came close to reproducing the data at all temperatures. The CaFe³⁺ excess term fits the data at 1400 and 1500°C but not at 1600°C. In view of the failure at 1600°C and considering the case for a CaSi excess term in the CaO-SiO₂ binary system (TOMLINSON *et al.*, 1958), we fit the volume data to an equation using both CaSi and CaFe³⁺ excess terms. The result (Table 5) was a successful description of the experimental data that returned reasonable volumes and expansivities for all the excess terms and partial molar volumes of the endmember oxides (see below).

The preferred fit—the CaSi and CaFe³⁺ excess terms

The preferred fit to the volume data of this study involves excess terms for Ca-Si and Ca-Fe³⁺. If this fit includes the correct number and form of significant excess terms to describe melt volumes in the investigated system fully, then comparison of the partial molar volumes of the endmember oxides with volume determinations on liquids of these endmember compositions is valid. We are aware of volume data for pure liquid SiO₂ (BACON *et al.*, 1960) and for extremely

reduced iron oxide (HENDERSON, 1964) in equilibrium with iron metal at 1410 and 1440°C. We are not aware of any liquid CaO or liquid Fe₂O₃ volume data. Similarly, we may take the partial molar volumes of previous fits to investigations in related systems and compare with pure endmember liquid volumes where known. This may be done in particular for Al₂O₃, (liquid Al₂O₃ volume data from KIRSCHENBAUM and CAHILL, 1960; MITLIN and NAGABIN, 1970), a component whose partial molar volume in silicate liquids has been compared with Fe₂O₃ by previous workers (*e.g.*, MO *et al.*, 1982; LANGE and CARMICHAEL, 1987) in attempts to derive structural information.

The partial molar volumes of SiO₂ derived from fit 4 to the data of this study, at 1400, 1500 and 1600°C may be compared with various other estimates of $V(\text{SiO}_2)$. The agreement between $V(\text{SiO}_2)$ from fit 4 and the extrapolation of the results of BACON *et al.*, (1960) is within mutual errors of these studies. In addition, the molar expansivities of SiO₂ agree well. The predicted value of $V(\text{SiO}_2)$ in this temperature range, if we (despite the warnings of the authors) extrapolate the multicomponent linear fitting models of MO *et al.* (1982), STEIN *et al.* (1986) and LANGE and CARMICHAEL (1987) to pure SiO₂, are also within the mutual experimental errors. However, we feel that the small thermal expansivity of SiO₂ derived from multicomponent linear fits of these authors may be an artifact of the inadequacy of a linear fit to describe fully the volumes of endmember liquids. The low partial molar thermal expansivity of SiO₂ derived by these authors might be supported by a low thermal expansivity of high quartz. (Note, however, that the compressibility of quartz is very different (lower) from that of vitreous silica, LEVIEN *et al.*, 1980.) We consider it reasonable that a liquid of SiO₂ composition whose basic structure is generally agreed to be six-membered rings of tetrahedra (*e.g.*, KONNERT and KARLE, 1973; TAYLOR and BROWN, 1979; NAVROTSKY *et al.*, 1982; SEIFERT *et al.*, 1982; HENDERSON *et al.*, 1984) should have a thermal expansivity similar to or larger than that of crystalline cristobalite. Comparison of the molar volume data of our preferred fit with that of cristobalite (see Table 9 of LANGE and CARMICHAEL, 1987) indicates that this is indeed the case.

The partial molar volume of Fe₂O₃ derived in fit 4 may be compared with the molar volume of crystalline Fe₂O₃ in the same temperature range. As noted above, previous workers have used the molar volume of crystalline Fe₂O₃ as an estimate of the partial molar volume of Fe₂O₃ in octahedral coordination. The values of $V(\text{Fe}_2\text{O}_3)$ derived from previous linear fits to multicomponent volume data sets have been consistently larger than the crystalline molar volume of Fe₂O₃ by about 30%. Similar comparisons have been made for Al₂O₃. The conclusion drawn from such comparisons has been that the partial molar volumes of Fe₂O₃ and Al₂O₃ obtained from the linear fits to the melt volume data imply a tetrahedral coordination of Al³⁺ and Fe³⁺ in these liquids. In the temperature range of this study, the partial molar volumes of Fe₂O₃ derived from fit 4 range from 0.89 to 0.99% of the value for crystalline Fe₂O₃. If the value for crystalline Fe₂O₃ may be used as an indication of the partial molar volume of octahedral Fe₂O₃ at these temperatures, then the values of $V(\text{Fe}_2\text{O}_3)$ obtained from fit 4 are clearly consistent with a melt structural endmember of octahedral Fe₂O₃.

The CaFe excess term is large, positive and decreases with temperature. If we infer that the origin of this positive excess term is due to complex formation involving Ca and Fe³⁺ to yield tetrahedral coordination of ferric iron in Ca_{0.5}FeO₂ tetrahedral complexes, and if the endmember partial molar volume of Fe₂O₃ represents octahedral coordination of Fe³⁺, then the decrease in the magnitude of this term with increasing temperature is consistent with a decrease in the stability of the Ca_{0.5}FeO₂ complex. This, in turn implies a decrease in the proportion of Fe³⁺ that is in tetrahedral coordination in these melts with increasing temperature. Such a temperature-dependence of the proportions of tetrahedral and octahedral ferric iron in these melts is consistent with the positive temperature-dependence of the ferric isomer shift obtained from single ferric doublet fits (Table 3a). Also, the temperature-dependence of ferric iron coordination can explain the negative temperature-dependence of the partial molar volume of Fe₂O₃ observed in the fits of Table 5 that exclude an excess term involving ferric iron, with or without a CaSi excess term. Finally, the general observation of increasing ferric isomer shift (and inferred coordination shift of ferric iron) with melt reduction (see MYSEN, 1988, for summary) suggests that the ferric isomer shift (and putative coordination shift) with increasing temperature is a simple consequence of the reduction of these melts with increasing temperature and is, therefore, to be expected. Additionally, MYSEN and VIRGO (1985) have observed equivalent behavior as a function of pressure for melts on the Na₂Si₂O₅-Fe₂O₃ join (*i.e.*, an increase of ferric iron isomer shift in the ⁵⁷Fe Mössbauer of melts that are reduced, in this case, due to increasing pressure).

The CaSi excess term is a small negative term that increases in magnitude with temperature from being negligible at 1400°C (within 1 standard error of zero) to being significantly negative at 1600°C. As noted above, negative CaSi excess terms were also determined to be necessary in fitting the molar volume data in the binary CaO-SiO₂ system (TOMLINSON *et al.*, 1958) and the ternary CaO-Al₂O₃-SiO₂ system (LANGE and CARMICHAEL, 1987). A simplistic explanation for the negative excess term is the volume decrease associated with mechanical mixtures of particles of unlike size. A larger excess term with increasing temperature might imply that a greater dispersion of polymerized species of differing sizes is occurring with temperature increase. This interpretation would be consistent with the evidence from ²⁹Si NMR of sodium disilicate glasses (BRANDISS and STEBBINS, 1987; STEBBINS, 1987) which indicate a positive quench-temperature-dependence of dispersion of Q species (*i.e.*, increase in the proportions of more (Q₄) and less (Q₂) polymerized silicate tetrahedra at the expense of intermediate species (Q₃)). Similarly, SEIFERT *et al.* (1981) reported high temperature Raman spectra of Na₂O-SiO₂ and Na₂O-Al₂O₃-SiO₂ melts. They inferred that the disproportionation of Q₃ units to Q₂ and Q₄ units is a positive function of temperature.

The partial molar volumes of FeO derived from fit 4 of Table 5 are higher than would be predicted from the linear fits of previous investigations of multicomponent silicate melts (see discussion in HERZBERG, 1987). Of greater interest to us is the discrepancy with the data of HENDERSON (1964) on pure iron oxide in equilibrium with iron metal. If we use our value of 28.44 cm³/mole for $V(\text{Fe}_2\text{O}_3)$ and calculate the

value of $V(\text{FeO})$ from HENDERSON (1964) at 1410°C, we obtain 16.01 cm³/mole. The values of $V(\text{FeO})$ at 1500°C and 1600°C, which are better constrained due to the higher FeO contents of our experimental liquids with increasing temperature, are within error of the value of $V(\text{FeO})$ derived from the above using a reasonable partial molar expansivity.

On closer inspection, however, several lines of evidence combine to suggest that the volume behavior of ferrous iron in silicate melts may be more complicated than can be described by a single partial molar volume of FeO in the absence of any excess terms involving ferrous iron. Firstly, Fig. 7 of SHIRAISHI *et al.* (1978) illustrates the large uncertainty in $V(\text{FeO})$ associated with the poor agreement between studies. Secondly, conflicting interpretations of the coordination of FeO in liquid silicates, *i.e.*, tetrahedral coordination (WASEDA *et al.*, 1980; WAYCHUNAS *et al.*, 1987) versus octahedral coordination (see MYSEN, 1988, for a review) may, in future, be resolved by a model involving a temperature- and/or compositional-dependence of Fe²⁺ coordination and the higher values of $V(\text{FeO})$ of fit 4 might be consistent with some tetrahedral coordination of Fe²⁺. Thirdly, anomalous compositional-dependence of densities (HENDERSON, 1964) and viscosities (*e.g.*, SHIRAISHI *et al.*, 1978) in FeO-rich (>60 mole%) silicate melts suggest complex structural reorganization in these liquids in the compositional vicinity of fayalite. Fourthly, and finally, the close link observed between the redox ratio and the increase in the value of ferric iron isomer shift in alkali and alkaline earth silicate glasses (*e.g.*, MYSEN, 1988) suggests that FeO plays some special role in the determination of Fe³⁺ coordination. If this is so, then an excess term involving FeO is expected to be required to fit the density data of more reduced melts in the CaO-FeO-Fe₂O₃-SiO₂ system. In light of the above, further comparisons involving $V(\text{FeO})$ are not warranted.

Implications for melt properties

The identification of a compositional-dependence of the partial molar volume of ferric iron in simple silicate melts at 1 atm raises several interesting possibilities and poses a number of questions that may be addressed experimentally. The quantitative generalization of the results of this study to natural silicate liquids, however, must pass a number of tests. Firstly, it must be demonstrated whether one or both of the coordination states of ferric iron dominate the composition range of natural silicate liquids. Perhaps the largest influence on the partial molar volume of ferric iron, not addressed to date, is the effect of Al₂O₃. One might anticipate that Al₂O₃ would reduce the stability of ferric iron in tetrahedral coordination. However, observations of the apparent partial molar volume of ferric iron that result from linear fits proposed to describe the volume data of multicomponent aluminosilicate melts yield apparent partial molar volumes of ferric iron that indicate tetrahedral coordination of ferric iron (*e.g.*, MO *et al.*, 1982; LANGE and CARMICHAEL, 1987). Much of the input data into these fits, however, are for melts which contain ferric iron or aluminum but not both. (Also recall the equivalence within error of values of $V(\text{Fe}_2\text{O}_3)$ obtained from linear fits to Na₂O-FeO-Fe₂O₃-SiO₂ and CaO-FeO-Fe₂O₃-SiO₂ volume data, above.) Densitometry in iron-bearing aluminosil-

icate melt systems is required to determine the effect of aluminum on the partial molar volume of Fe₂O₃.

Even though we have demonstrated a compositional-dependence of the partial molar volume of ferric iron in melts in the CaO-FeO-Fe₂O₃-SiO₂ system, it may turn out that a linear fit to multicomponent melts will remain adequate for describing the densities of 1 atm aluminosilicate melts. We appreciate the possibility that the effects observed herein may be insignificant for such calculations (the significance remains to be tested.) However, even if this is the case, the evidence of different coordination states of ferric iron, which cannot, by definition, be derived from a linear fit to 1 atm volume data, may have very important implications for other partial molar properties of ferric iron in silicate melts. One of the most obvious possibilities concerns the effect of a tetrahedral-octahedral ferric iron coordination transfer on melt compressibility. Much has been written concerning the possibilities of coordination transformations of Al and Fe³⁺ in silicate melts at high pressure (WAFF, 1975; KUSHIRO, 1976; OHTANI *et al.*, 1985; FLEET *et al.*, 1984; MYSEN and VIRGO, 1985) including a significant effect expected for partial molar compressibilities (and bulk melt compressibility). If the composition range of igneous melts spans a coordination shift of ferric iron, then the partial molar compressibility of ferric iron in silicate melts may vary strongly from low values in 1 atm melts containing octahedrally-coordinated ferric iron to high values in melts containing tetrahedrally-coordinated ferric iron. Thus, the pressure dependence of redox equilibria in natural silicate melts may depend strongly on bulk composition. This would have implications for calculations involving the redox conditions of source regions based on erupted lava, melt redox, data. Compressibility data for ferric iron-bearing melts are badly needed and could be obtained from buffered, redox equilibria experiments at high pressure or from 1 atm ultrasonic interferometry measurements.

Just as it is likely that the pressure-dependence of redox equilibria in silicate melts is a strong function of the coordination number of ferric iron (due to the large observed difference in partial molar volumes), so it is possible that the temperature-dependence of redox equilibria varies with the coordination of ferric iron. Inspection of the redox data of this study for a wide range of CaO-FeO-Fe₂O₃-SiO₂ melt compositions indicates that the temperature-dependence of the redox ratio is a function of composition. Similarly, a least-squares fit to the combined redox equilibria data of BOWEN *et al.* (1933), PHILLIPS and MUAN (1959) and KRESS and CARMICHAEL (1988) for melts in the CaO-FeO-Fe₂O₃-SiO₂ system indicate a nonlinear relationship between $\log(\text{Fe}^{3+}/\text{Fe}^{2+})$ and $\log f\text{O}_2$ (KRESS and CARMICHAEL, 1988). These two observations can be reconciled by a redox enthalpy which varies with ferric iron coordination. Such an effect may be possible to observe using high temperature, redox equilibria in a gas-mixing calorimeter.

Finally, we wish to emphasize that the present understanding of ferrous iron in these melts and its relationship to ferric iron coordination is not fully understood. Ferrous iron may be the most important variable in determining ferric iron coordination, as evidenced by the tight control that the redox ratio appears to have in determining the shift of the ferric ⁵⁷Fe Mössbauer parameters (MYSEN, 1988). Conflicting

coordination assignments of ferrous iron may yet be brought into agreement by a model incorporating a compositional-dependence of ferrous iron coordination. Accordingly, we are reluctant to ascribe all nonlinearity in iron redox behavior to ferric iron.

SUMMARY

The compositional dependence of liquid volumes in the $\text{CaO-FeO-Fe}_2\text{O}_3\text{-SiO}_2$ system is a nonlinear function of the oxide components (*i.e.*, the partial molar volume of ferric iron is dependent on composition). A large positive excess term observed, involving Ca and Fe^{3+} , is consistent with the formation $\text{Ca}_0.5\text{FeO}_2$ complexes where Ca stabilizes the tetrahedral coordination of ferric iron. The negative temperature-dependence of this excess term implies decreasing stability of the tetrahedral complex with increasing temperature and this trend is supported by a positive quench-temperature dependence of the isomer shift of the ferric iron component of ^{57}Fe Mössbauer spectra of glasses in this system. The end-member partial molar volume of ferric iron is consistent with octahedral coordination of ferric iron in liquid Fe_2O_3 . This evidence for two coordination states of ferric iron in silicate melts whose proportions vary as a function of temperature, pressure and composition implies that ferric iron should be treated as two separate components in calculation of melt properties. The presence of two ferric iron species is expected to affect the temperature-, pressure- and compositional-dependence of redox equilibria. The compositional-dependence of other partial molar properties of ferric iron in silicate melts remains to be investigated.

Acknowledgements—We wish to thank Kurt Klasinski and Georg Herrmannsdörfer for technical support and Fritz Seifert for discussions. We thank R. A. Lange and C. Herzberg for helpful reviews. Brearley acknowledges support from NSF grants EAR87-05870 and EAR87-20289 to A. Montana.

Editorial handling: P. C. Hess

REFERENCES

- BACON J. F., HASAPIS A. A. and WHOLLEY J. W. JR. (1960) Viscosity and density of molten silica and high silica content glasses. *Phys. Chem. Glasses* **1**, 90–98.
- BOTTINGA Y., RICHEL P. and WEILL D. (1983) Calculation of the density and thermal expansion coefficient of silicate liquids. *Bull. Mineral.* **106**, 129–138.
- BOTTINGA Y., WEILL D. and RICHEL P. (1984) Density calculations for silicate liquids: Reply to a Critical Comment by Ghiorsio and Carmichael. *Geochim. Cosmochim. Acta* **46**, 909–919.
- BOWEN N. L., SCHAIRER J. F. and WILLEMS H. W. V. (1930) The ternary system $\text{NaSiO}_3\text{-Fe}_2\text{O}_3\text{-SiO}_2$. *Amer. J. Sci.* **20**, 405–455.
- BOWEN N. L., SCHAIRER J. F. and POSNJAK E. (1933) The system CaO-FeO-SiO_2 . *Amer. J. Sci.* **26**, 193–284.
- BRANDISS M. E. and STEBBINS J. F. (1987) Effects of glass transition temperature on silicate glass structures: Variations in Q-species abundances (abstr.). *Eos* **68**, 1456.
- BROWN G., KEEFER K. D. and FENN P. M. (1979) Extended X-ray absorption fine structure of iron-bearing silicate glasses: Iron coordination environment and oxidation state. *Geol. Soc. Amer. Abstr. Prog.* **11**, 373.
- DANCKWERTH P. A. and VIRGO D. (1982) Structural state of iron in the system $\text{Na}_2\text{O-SiO}_2\text{-Fe-O}$. *Carnegie Inst. Wash. Yearb.* **81**, 340–342.
- DICKENSON M. P. and HESS P. C. (1986) The structural role and homogeneous redox equilibria of iron in peraluminous, metaluminous and peralkaline silicate melts. *Contrib. Mineral. Petrol.* **92**, 207–217.
- DINGWELL D. B. and VIRGO D. (1987) The effect of oxidation state on the viscosity of melts in the system $\text{Na}_2\text{O-FeO-Fe}_2\text{O}_3\text{-SiO}_2$. *Geochim. Cosmochim. Acta* **51**, 195–205.
- DINGWELL D. B. and VIRGO D. (1988) Contrasting viscosity-oxidation state trends in “hedenbergite” melt and the coordination transformation of ferric iron. *Geochim. Cosmochim. Acta* (submitted).
- DINGWELL D. B., BREARLEY M. and DICKINSON J. E. JR. (1988) Melt densities in the $\text{Na}_2\text{O-FeO-Fe}_2\text{O}_3\text{-SiO}_2$ system and the partial molar volume of tetrahedrally-coordinated ferric iron in silicate melts. *Geochim. Cosmochim. Acta* **52**, 2467–2475.
- FLEET M. E., HERZBERG C. T., HENDERSON G. S., CROZIER E. D., OSBORNE M. D. and SCARFE C. M. (1984) Coordination of Fe, Ga and Ge in high pressure glasses by Mössbauer, Raman and X-ray absorption spectroscopy, and geological implications. *Geochim. Cosmochim. Acta* **48**, 1455–1466.
- FOX K. E., FURUKAWA T. and WHITE W. B. (1982) Transition metal ions in silicate melts. Part 2. Iron in sodium silicate glasses. *Phys. Chem. Glasses* **32**, 169–173.
- FRISCHAT G. H. and TOMANDL G. (1968) Mößbaueruntersuchung von Wertigkeitsverhältnis und Koordination des Eisens in Silicatgläsern. *Glastechn. Ber.* **41**, 182–185.
- GOLDMAN D. S. (1986) Evaluation of the ratios of bridging to non-bridging oxygens in simple silicate glasses by electron spectroscopy for chemical analysis. *Phys. Chem. Glasses* **27**, 128–133.
- HENDERSON J. (1964) Density of lime-iron oxide-silica melts. *Trans. Met. Soc. AIME* **230**, 501–504.
- HENDERSON G. S., FLEET M. S. and BANCROFT G. M. (1984) An X-ray scattering investigation of vitreous KFeSi_3O_8 and $\text{NaFeSi}_3\text{O}_8$ and re-investigation of vitreous SiO_2 using quasicrystalline modelling. *J. Non-Cryst. Solids* **68**, 333–349.
- HERZBERG C. (1987) Magma density at high pressure. Part 2: A test of the olivine flotation hypothesis. In *Magmatic Processes: Physicochemical Principles* (ed. B. O. MYSEN); *Geochem. Soc. Spec. Publ.* **1**, 47–58.
- JANZ G. J. (1980) Molten salts data as reference data for density, surface tension, viscosity and electrical conductance: KNO_3 and NaCl . *J. Phys. Chem. Ref. Data* **9**, 791–829.
- KIRSCHENBAUM A. D. and CAHILL J. A. (1960) Density of liquid aluminum oxide. *J. Inorg. Nucl. Chem.* **14**, 283–287.
- KONNERT J. H. and KARLE L. (1973) The computation of radial distribution functions for glassy materials. *Acta Crystal.* **29**, 702–710.
- KRESS V. C. and CARMICHAEL I. S. E. (1988) Experimental investigation of the oxidation state of melts in the system $\text{CaO-FeO-Fe}_2\text{O}_3\text{-SiO}_2$ (abstr.). *Eos* **69**, 512.
- KURKJIAN C. R. and SIGETY C. R. (1968) Co-ordination of Fe^{3+} in glass. *Phys. Chem. Glasses* **9**, 73–83.
- KUSHIRO I. (1976) Changes in the viscosity and structure of melt of $\text{NaAlSi}_2\text{O}_6$ composition at high pressures. *J. Geophys. Res.* **81**, 6347–6350.
- LANGE R. A. and CARMICHAEL I. S. E. (1987) Densities of $\text{Na}_2\text{O-K}_2\text{O-CaO-MgO-FeO-Fe}_2\text{O}_3\text{-Al}_2\text{O}_3\text{-TiO}_2\text{-SiO}_2$ liquids: New measurements and derived partial molar properties. *Geochim. Cosmochim. Acta* **51**, 2931–2946.
- LARSON H. and CHIPMAN J. (1953) Oxygen activity in iron oxide slags. *Trans. AIME* **197**, 1989–1093.
- LEVIEN L., PREWITT C. T. and WEIDNER D. J. (1980) Structure and elastic properties of quartz at pressure. *Amer. Mineral.* **65**, 920–930.
- LEVY R. A., LUPIS C. H. P. and FLINN P. A. (1976) Mössbauer analysis of the valence and coordination of iron cations in $\text{SiO}_2\text{-Na}_2\text{O-CaO}$ glasses. *Phys. Chem. Glasses* **17**, 94–103.
- LICKO T., DANEK V. and PANEK Z. (1985) Densities of melts in the system $\text{CaO-FeO-Fe}_2\text{O}_3\text{-SiO}_2$. *Chem. Papers* **39**, 599–605.
- MAO H-K., VIRGO D. and BELL P. M. (1973) Analytical study of the orange lunar soil returned by the Apollo 17 astronauts. *Carnegie Inst. Wash. Yearb.* **72**, 631–638.
- MITLIN B. S. and NAGABIN YU. A. (1970) Density of molten aluminum oxide. *Russ. J. Phys. Chem. (Engl. Trans.)* **44**, 741–742.
- MO X., CARMICHAEL I. S. E., RIVERS M. and STEBBINS J. (1982)

- The partial molar volume of Fe₂O₃ in multicomponent silicate liquids and the pressure dependence of oxygen fugacity in magmas. *Mineral. Mag.* **45**, 237–245.
- MYSEN B. O. (1988) Relation between structure, redox equilibria of iron and properties of magmatic liquids. In *Advances in Physical Geochemistry* (eds. I. KUSHIRO and L. PERCHUK), in press.
- MYSEN B. O. and VIRGO D. (1983) Iron-bearing alkaline-earth silicate melts: relations between redox equilibria of iron, melt structure, and liquidus phase equilibria. *Carnegie Inst. Wash. Yearb.* **82**, 317–321.
- MYSEN B. O. and VIRGO D. (1985) Iron-bearing silicate melts: relations between pressure and redox equilibria. *Phys. Chem. Mineral.* **12**, 191–200.
- MYSEN B. O., SEIFERT F. A. and VIRGO D. (1980) Structure and redox equilibria of iron-bearing silicate melts. *Amer. Mineral.* **65**, 867–884.
- MYSEN B. O., VIRGO D. and SEIFERT F. A. (1984) Redox equilibria of iron in alkaline earth silicate melts: relationships between melt structure, oxygen fugacity, temperature and properties of iron-bearing silicate liquids. *Amer. Mineral.* **69**, 834–847.
- MYSEN B. O., VIRGO D., NEUMANN E. and SEIFERT F. (1985) Redox equilibria and the structural states of ferric and ferrous iron in melts in the system CaO-MgO-Al₂O₃-SiO₂-Fe-O: Relationships between redox equilibria, melt structure and liquidus phase equilibria. *Amer. Mineral.* **70**, 317–331.
- NAVROTSKY A., PERADEAU G., MCMILLAN P. and COUTURES J-P. (1982) A thermochemical study of glasses and crystals along the joins silica-calcium aluminate and silica-sodium aluminate. *Geochim. Cosmochim. Acta* **46**, 2039–2047.
- OHTANI E., TAULELLE F. and ANGELL C. A. (1985) Al³⁺ coordination changes in aluminosilicate liquids under pressure. *Nature* **314**, 78–81.
- OSBORN E. F. and MUAN A. (1960) *Phase Equilibrium Diagrams of Oxide Systems. The System CaO-Al₂O₃-SiO₂*. American Ceramic Society, Columbus, Ohio.
- PARGAMIN L., LUPIS C. H. P. and FLINN P. A. (1972) Mössbauer analysis of the distribution of iron cations in silicate slags. *Metall. Trans.* **3**, 2093–2105.
- PHILLIPS B. and MUAN A. (1959) Phase equilibria in the system CaO-iron oxide-SiO₂ in air. *J. Amer. Ceram. Soc.* **42**, 413–423.
- SCHAIRES J. F. and BOWEN N. L. (1956) The system Na₂O-Al₂O₃-SiO₂. *Amer. J. Sci.* **256**, 129–195.
- SEIFERT F., MYSEN B. O. and VIRGO D. (1981) Similarity of glasses and melts relevant to petrological processes. *Geochim. Cosmochim. Acta* **45**, 1879–1884.
- SEIFERT F., MYSEN B. O. and VIRGO D. (1982) Three-dimensional network structure of quenched melts (glass) in the systems SiO₂-NaAlO₂, SiO₂-CaAl₂O₄ and SiO₂-MgAl₂O₄. *Amer. Mineral.* **67**, 696–717.
- SHIRAIISHI Y., IKEDA K., TAMURA A. and SAITO T. (1978) On the viscosity and density of the molten FeO-SiO₂ system. *Trans. Jap. Inst. Metal.* **19**, 264–274.
- STEBBINS J. (1987) Identification of multiple structural species in silicate glasses by ²⁹Si NMR. *Nature* **330**, 465–467.
- STEIN D. J., STEBBINS J. F. and CARMICHAEL I. S. E. (1986) Density of molten sodium aluminosilicates. *J. Amer. Ceram. Soc.* **69**, 396–399.
- TAYLOR M. and BROWN G. E. (1979) Structure of mineral glasses II. The SiO₂-NaAlSiO₄ join. *Geochim. Cosmochim. Acta* **43**, 1467–1475.
- TOMLINSON J. W., HEYNES M. S. R. and BOCKRIS J. O'M. (1958) The structure of liquid silicates: Part 2—molar volumes and expansivities. *Trans. Faraday Soc.* **54**, 1822–1833.
- VIRGO D. and MYSEN B. O. (1985) The structural state of iron in oxidized versus reduced glasses at 1 atm: a ⁵⁷Fe Mössbauer study. *Phys. Chem. Mineral.* **12**, 65–76.
- WAFF H. S. (1975) Pressure-induced coordination changes in magmatic liquids. *Geophys. Res. Lett.* **2**, 193–196.
- WASEDA Y., SHIRAIISHI Y. and TOGURI J. M. (1980) The structure of the molten FeO-Fe₂O₃-SiO₂ system by X-ray diffraction. *Trans. Jap. Inst. Metals* **21**, 51–62.
- WAYCHUNAS G. A., BROWN G. E., PONADER C. W. and JACKSON W. E. (1987) EXAFS study of molten alkali silicates: evidence for network forming Fe²⁺ (abstr.) *Mater. Res. Soc. Prog. Abstr.* Spring 1987, p. 296.